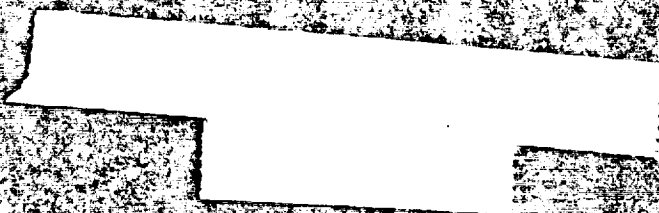
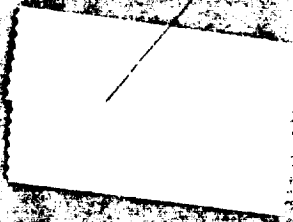


NACA-TN-892



TECHNICAL NOTES  
NATIONAL ADVISORY COMMITTEE FOR AERONAUTICS

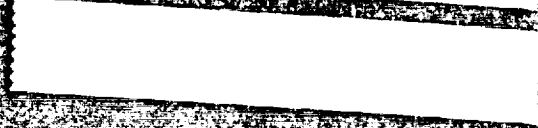
NACA-TN-892

No. 892

TURBULENT FLOW BETWEEN ROTATING CYLINDERS

by PAI-SHIH-I

California Institute of Technology



Washington  
March 1943

REPRODUCED BY  
NATIONAL TECHNICAL  
INFORMATION SERVICE  
U. S. DEPARTMENT OF COMMERCE  
SPRINGFIELD, VA. 22161



# NATIONAL ADVISORY COMMITTEE FOR AERONAUTICS

TECHNICAL NOTE NO. 892

## TURBULENT FLOW BETWEEN ROTATING CYLINDERS

By Pai Shih-I

### SUMMARY

The turbulent air flow between rotating coaxial cylinders was investigated. The distributions of mean speed and of turbulence were measured in the gap between a rotating inner and a stationary outer cylinder.

The measurements led to the conclusion that the turbulent flow in the gap cannot be considered two-dimensional but that a peculiar type of secondary motion takes place. It is shown that the experimentally found velocity distribution can be fully understood under the assumption that this secondary motion consists of three-dimensional ring-shape vortices. The vortices occur only in pairs and their number and size depend on the speed of the rotating cylinder; the number was found to decrease with increasing speed. The secondary motion has an essential part in the transmission of the moment of momentum. In regions where the secondary motion is negligible, the momentum transfer follows the laws known for homologous turbulence.

Ring-shape vortices are known to occur in the laminar flow between rotating cylinders, but it was hitherto unknown that they exist even at speeds which are several hundred times the critical speed.

### INTRODUCTION

The flow between coaxial rotating cylinders is known as Couette's type of curved flow. Owing to the importance of this type of flow as a basic problem in fluid dynamics, a number of investigations have been carried out. The exact velocity distribution in the turbulent state, however, is still unknown. The flow was investigated by G. I. Taylor (references 1, 2, 3) as well as by others. (See, for example, reference 4.) Taylor measured the velocity distribution between a rotating inner and a stationary outer cylinder (reference 3). He found the paradoxical result that

both the circumferential velocity and the moment of momentum increase outward. This condition is apparently contrary to both of the alternative assumptions that the moment of momentum or the vorticity is transferred by turbulent diffusion. Taylor tried to explain this paradox by the shadow effect of the tube that was used for measuring the total-pressure distribution in the gap. He varied the dimensions of the instrument and concluded, by extrapolation to zero diameter of the pressure tube, that the true velocity distribution in the gap corresponded to a constant value of the moment of momentum, that is, to a constant value of the product  $Ur$  where  $U$  is the mean circumferential velocity and  $r$  is the distance from the axis of the cylinders.

In order to investigate the validity of Taylor's extrapolation, Dr. von Kármán suggested the use of hot-wire anemometers for the measurement of the velocity distribution. A special measuring device was designed to reduce the shadow effect to a negligible amount. The inner cylinder was rotated and the outer one held stationary. The operating speeds were several hundred times the critical speed as given by Taylor (reference 1).

The author wishes to express his thanks for the help received from the GALT staff, particularly to Dr. von Kármán for his inspiration and guidance, to Dr. C. B. Millikan for his interest and advice, and to Mr. Carl Thiele for his help and suggestions regarding apparatus. The section of the paper on theoretical discussion was contributed by Dr. von Kármán. This investigation, conducted at the California Institute of Technology, was sponsored by and conducted with the financial assistance of the National Advisory Committee for Aeronautics.

#### SYMBOLS

$r$ $\theta$ $z$	orthogonal, cylindrical coordinates
$l$	length of rotating cylinders
$t$	width of gap between cylinders
$R_1$	radius of outer cylinder
$y$	normal distance from a solid wall in logarithmic velocity distribution law

## DESCRIPTION OF APPARATUS

The inner cylinder was turned by a 1/10-horsepower synchronous motor coupled rigidly to its shaft. The speed of rotation of the cylinder was measured by means of a 10-pole generator attached to the motor shaft. The output of the generator was checked against that of a calibrated oscillator by the Lissajou figures formed on a cathode-ray oscilloscope.

A conventional hot-wire anemometer was used for the measurement of the mean velocity and the root mean square of the fluctuations of the magnitude of the velocity. The ratio between the root-mean-square of the fluctuation and the mean velocity multiplied by 100 will be referred to as the "percentage of turbulence." No attempt was made to determine the direction of the velocity.

The hot wire was inserted at the central part of the outer cylinder by the holder shown in figure 1. The hot wire was soldered across the small gaps and the small spindles could be changed so as to measure at different axial positions. The spindles were far from the hot wire and the effect of their wake was therefore negligible. The spindles were mounted on a block that rested on a slide so that the spindles could travel back and forth with the block as a whole. The slide was moved by a micrometer that indicated the position of the hot wire in the space between the cylinders.

A series of static holes, 15 in number, were drilled along an element of the outer cylinder. These static holes gave an indication of the flow pattern in the gap. Figure 2 shows the test setup with the hot-wire holder inserted in the center of the outer cylinder. The synchronous motor and the speed indicator are beneath the cylinder. The multiple stopcock on the stool permitted any desired static orifice to be connected to a manometer.

The front part of the hot-wire holder was made of hard rubber. In order to obtain a good fit between the hot-wire holder and the cylinder, a brass slot was made and set into the wall of the outer cylinder. The inside of the outer cylinder, the brass slot, and the hard rubber holder were turned as a unit and painted simultaneously. The three pieces formed a smooth cylindrical surface.

#### THEORETICAL DISCUSSION

Two different theories have been proposed for the computation of the velocity distribution in turbulent flow:

1. According to the momentum transport theory originated by L. Prandtl, the shearing stress  $\tau$  is given by the expression,

$$\tau = \frac{k}{r} \frac{d}{dr} (Ur),$$

where  $k$  denotes the coefficient of turbulent exchange,  $U$  is the circumferential velocity of the fluid, and  $r$  is the distance from the cylinder axis.

In the case of the flow between a rotating inner and a stationary outer cylinder, the moment of the shearing stresses acting on an arbitrary cylindrical layer in the fluid is equal to the moment required to rotate the inner cylinder. The moment referred to unit length being denoted by  $g$ , the equation takes the form

$$\tau r^2 = kr \frac{d}{dr} (Ur) = -g \quad (1)$$

It follows that the product  $Ur$  should decrease with increasing  $r$ .

2. According to the vorticity-transport theory originated by G. I. Taylor, the vorticity transport through any cylindrical surface is zero. The mathematical expression for this statement is

$$\frac{d}{dr} \left[ \frac{1}{r} \frac{d}{dr} (Ur) \right] = 0 \quad (2)$$

This equation is, for example, satisfied if  $Ur$  is constant. Taylor concluded from his measurements that  $Ur$  is, in fact, constant in the central 80 percent of the gap. As mentioned before, this conclusion was drawn from a special extrapolation; the investigations presented in this paper were undertaken mainly to clarify this point.

Preliminary measurements that are described in the following section of this paper showed that the flow between the cylinders was not two-dimensional as assumed in equations (1) and (2). The flow could be considered to consist of three parts: 1. The two-dimensional mean motion having but one circumferential velocity component; 2. A secondary motion which accounts for the deviation from the two-dimensional case; and 3. Turbulent fluctuations. General equilibrium conditions applied to this case require that the transfer of angular momentum through a cylindrical surface of radius  $r$  equal the torque, which is independent of  $r$ . Thus, if the stresses due to viscosity are neglected,

$$\int_0^l \int_0^{2\pi} r^2 (U + u + u') (v + v') dz d\theta = \text{constant} \quad (3)$$

where  $U$  is the mean circumferential velocity;  $u$  and  $v$  are the circumferential and radial components, respectively, of the secondary motion (that is, the deviation from the mean velocity);  $u'$  and  $v'$  are the components of the turbulent fluctuations in circumferential and radial direction;  $l$  is the length of the cylinder; and  $r$ ,  $\theta$  and  $z$  are cylindrical coordinates.

If averages with respect to time and over the length of the cylinder are made, it being assumed that the average values do not depend on  $\theta$ , it follows from equation (3) that

$$r^2 (\overline{uv} + \overline{u'v'}) = \text{constant} \quad (4)$$

since  $\overline{uv}$  vanishes by averaging over the length of the cylinder, because the continuity of the flow and the time averages of  $u'$  and  $v'$  are zero by definition. This equation shows that the torque is transferred from one cylinder to the other by two different mechanisms: one, secondary motion and, two, turbulent fluctuations. The relative importance of these motions was to be experimentally determined. It is to be noted that equation (3) is quite general and does not depend on any assumption as to the mechanism of the turbulent friction.

#### PRELIMINARY INVESTIGATION

At first it was thought that the flow between the cylinders would be two-dimensional except near the ends. Measurements were therefore made at the exact center of the cylinders where the flow would best approximate the two-dimensional type. Two entirely distinct types of flow were, however, obtained at the same position, depending on the starting conditions. The typical sets of the velocity and the distributions of the turbulence level across the gap for these two types of flow are shown in figures 3 to 6. For convenience, the type of flow shown in figures 3 and 5 will be called type A and that shown in figures 4 and 6 will be called type B.

The relation of these two types of flow to the starting conditions was as follows:

If the inner cylinder was started in such a manner that its speed  $N_1$  increased gradually up to the desired value and if the hot-wire spindles were close to the inner



cylinder, type A flow was obtained. Once either type of flow was established it seemed unaffected by slight changes in speed of rotation.

Furthermore, at high speeds it was found that in the middle of the run the type A flow might suddenly change to the type B flow. This change is illustrated in figure 7. At first the cylinders were started in such a way that the type A flow was obtained, and readings were taken outward. These readings followed the upper full-line curve as shown in figure 7. At a certain point near the outer wall, the mean speed suddenly dropped along the dotted line and the velocity distribution then became that shown in the lower full-line curve, that is, type B flow. Further traversing had no effect on the flow pattern. When the  $17/32$ -inch gap was used, decreasing the speed of rotation of the inner cylinder to a certain low value restored the type A flow. This phenomenon, however, did not occur for the  $1\frac{1}{16}$ -inch gap.

It was believed that the presence of the hot wire near the inner or the outer cylinder could have an essential influence on the velocity distribution, for example, by increasing the thickness of the boundary layer. This possibility was excluded by introducing a dummy hot wire at various positions. The next assumption was that the flow pattern is three-dimensional; the transitions between the two types of velocity distribution would be caused by changes or displacements in the flow pattern. This assumption was confirmed by further experiments.

In order to investigate the three-dimensional character of the flow in the gap between the cylinders, evenly spaced pressure-measuring orifices were inserted on the outer cylinder along the axial direction. The readings at these orifices (fig. 8) showed that the static pressure was not constant along the axial direction, as would have been expected in the case of two-dimensional flow, but showed systematic variations.

The end conditions of the cylinders were found to have considerable influence on the static-pressure readings. In order to eliminate the end effect as far as possible, the "aspect ratio," that is, the length of the working section to the width of the gap, was increased from 10 to 20 by reducing the gap from  $1\frac{1}{16}$  inches to  $17/32$  inch. The seals at the two ends of the gap were also redesigned to make the end conditions as symmetrical as possible. The pressure and the velocity distributions obtained with the

symmetrical seals were similar for the two aspect ratios, and it is believed that the end effects were negligible at the place where the measurements were taken.

Thus, the measurements of the static pressure indicate without doubt the three-dimensional character of the flow. In order to determine the flow pattern, it became necessary to measure the velocity distribution in various sections perpendicular to the axis. These measurements are described in the next section.

#### VELOCITY AND TURBULENCE DISTRIBUTIONS ALONG THE AXIAL DIRECTION OF THE CYLINDERS

Since the flow pattern could be changed by the starting conditions, care had to be exercised that the static-pressure distribution along the axial direction was kept the same for all the runs at any given speed. Measurements were taken at seven axial stations at the central portion of the cylinders. The distance between two adjoining stations was  $1/2$  inch. These stations were numbered from 1 to 7, the number increasing toward the bottom of the cylinders. The actual positions of these stations are marked by the arrows in the static-pressure diagrams, on the right of the corresponding results.

A typical set of results, corresponding to a rotational speed of the inner cylinder equal to 1200 rpm will be analyzed in detail.

The mean-velocity distributions for this case are shown in figure 9. It is seen that both types of flow obtained in the preliminary investigations existed simultaneously for the same flow pattern but at different axial positions. The mean-velocity distribution gradually changes from one type to the other. For instance, at station 1 the distribution is type B; at stations 2 and 3, it is type A; at station 4, it is an intermediate type, and it may be called  $A_B$ ; at stations 5 and 6, it is type B; while at station 7, the intermediate stage is again obtained.

Figure 10 was obtained by plotting one of the distributions of type A, say at station 2, and one of type B, say at station 6, on a semilogarithmic scale. It is seen from these curves that, for flow of type A, the velocity

distribution near the inner wall is logarithmic, that is, the velocity defect is proportional to the logarithm of the distance from the wall (reference 5); whereas, for type B, the velocity distribution near the outer wall is logarithmic. If the typical velocity distributions obtained in the preliminary investigations are plotted in the same manner, the results are similar. It has been shown by Dr. von Kármán (reference 6) that for Couette's flow the mean-velocity distribution is logarithmic if homologous turbulence is assumed. It may be stated that, at the place where the velocity distribution is logarithmic, the transfer of shearing stress from one cylinder to the other is mainly due to turbulent fluctuations.

Since the gap is small in comparison with the radii of both cylinders, as a first approximation, equation (4) gives

$$\overline{uv} + \overline{u'v'} = \text{constant} \quad (5)$$

At the place where the influence of the secondary motion, that is, the term of  $\overline{u'v'}$ , is negligible, equation (5) becomes

$$\overline{u'v'} = \text{constant} \quad (6)$$

The same condition is valid for flow between two parallel plates moving with different velocities.

At the place where the influence of turbulent fluctuations is small, equation (5) becomes

$$\overline{uv} = \text{constant} \quad (7)$$

No attempt was made to measure the radial velocity  $v$  of the secondary motion. Some conclusions as to the distribution of  $v$  along the axial direction can be drawn, however, from equation (7) after the distribution of  $u$  is examined, that is, the deviation of the circumferential velocity from the average taken over the axial length.

First, take the average of the mean-velocity curves of the seven stations. This average mean-velocity distribution is plotted as a dotted curve for comparison with the curves of mean-velocity distribution of figure 9. The deviation  $u$  from the average distribution at various axial positions is shown in figure 11.

It is seen from equation (7) that, if  $u$  changes sign along the axis of the cylinder,  $v$  must also change sign since the product is a constant. But from figure 10 it is seen that, for flow of type A,  $u$  is positive and that, for type B,  $u$  is negative. Hence, it can be concluded that the radial component  $v$  of the velocity of the secondary motion changes its direction with the type of flow. At stations where the velocity-distribution curve shows type A, the radial velocity is directed outward; while at stations where the velocity distribution is of type B, the radial velocity is directed inward.

### RING-SHAPE VORTICES

It seems, therefore, that ring-shape vortices which are known to introduce the instability of the flow in rotating cylinders still exist at Reynolds numbers as high as several hundred times the critical Reynolds number. In order to give a satisfactory explanation of the experimental results, these ring-shape vortices must be assumed to be distorted and arranged as shown in figure 12. (Cf. reference 1 in which Taylor's original conception of the vortices is given.) The fluid along the walls diverges from station 3 and from a point that lies somewhat beyond station 7. It has been found that the pressure has peaks at these points. The static pressure drops in the neighborhood of stations 3 and 7 rather rapidly, and over the mean portion of the interval between the two peaks the static pressure is more or less constant. Near the walls, the fluid flows in the direction of decreasing pressure; where the pressure is constant, there is practically no flow in the axial direction. This result is consistent with the suggested distribution of the vortices. Opposite stations 2 and 3 near the inner cylinder there is a purely turbulent domain. In this turbulent domain, the velocity distribution is expected to be logarithmic; this expectation has been found to be correct. At stations 5 and 6, where the velocity distribution is of type B, there is a purely turbulent domain near the outer cylinder wall. At stations 4 and 7, the intermediate stage will be obtained because the influence of the secondary motion and that of the turbulent fluctuations are of the same order of magnitude.

Very close to the walls, the shear should be mainly determined by pure viscosity. In order to transmit the same amount of shear as exists in the central portion of

the gap, the slope of the velocity curve near the walls must be very large. In all the velocity curves obtained, this result is true.

The distributions of  $u'$ , the circumferential turbulent fluctuations, are shown in figure 13. It is interesting to note that the curvature of the distribution curves for  $u$  and  $u'$  are opposite for any given axial position.

In order to find the influence of the speed of rotation on the vortices, measurements at a fixed axial position but with different rotation speed were made. The results are plotted in figure 14. At the low speed of 1200 rpm, the curve shown as diagram 1 of figure 14 was obtained. It shows essentially a flow of type A. The speed was then increased to 1500 and 1800 rpm. The results are given in diagrams 2 and 3, respectively. The distribution of the static pressure as well as the distribution of the mean velocity are more or less similar to those of diagram 1. Finally the speed was increased to 2100 rpm. The distributions of the static pressure and of the mean velocity were suddenly changed, as shown in diagram 4. The pressure peak that existed in the three preceding cases at the midpoint, where the measurements were taken, disappeared, and thus the mean-velocity distribution at this point became of type B. When the speed was reduced to 1800 and 1500 rpm, diagrams 5 and 6 were obtained. They are similar to diagram 4, which shows that the new flow pattern, once established, continued after a considerable reduction of the speed. As the speed of rotation was reduced to 1200 rpm, however, the original flow pattern returned, as shown in diagram 7.

At lower speed there seemed to be a certain stable configuration involving a definite size and number of the vortices. As the speed was increased, a critical value was reached at which the vortices increased in size and decreased in number. Since the vortices can exist only in pairs, because the total circulation must be zero, a pair of vortices must disappear at a certain critical speed as the speed increases and reappear at some critical speed as the speed decreases. It seems that these two critical speeds are not identical. This mechanism fully explains the sudden changes of the flow encountered in the preliminary investigations. The effect of the position of the spindles probably consists of the delaying of the change in the number of vortices. When the spindles were situated in a purely turbulent domain, however, their influences were eliminated. This result is consistent with the experimental results.

Only two stable vortex-system configurations were observed. One consisted of six vortices and the other of four vortices. The one that prevailed at the lower speed is called the small-vortex system and that existing at high speed, the large-vortex system. For the 17/32-inch gap the upper critical speed of the small-vortex system was found at 1800 rpm or higher. Hence, the upper limit of the critical Reynolds number for the existence of the small-vortex system is about 200 times the critical Reynolds number for the instability of the laminar flow. Beyond this limit only the large-vortex system can exist. The lower limit of the critical Reynolds number for the large-vortex system, that is, at 1200 rpm or lower, is about 100 times that of the critical Reynolds number for the instability of the laminar flow. Below this limit only the small-vortex system can exist. There is a range in which both types of the flow pattern can exist, and the starting conditions determine which pattern prevails in a particular case. For the 1 1/8-inch gap the lowest operating Reynolds number was about 175 times that of the critical Reynolds number and a change could be made from the large-vortex system to the small-vortex system if the large-vortex system was once established.

#### ESTIMATE OF SHEARING STRESSES

The shearing stress can be estimated from the logarithmic velocity profile by assuming that the relations obtained for parallel flow are also valid in this case. By the well-known universal velocity distribution near the wall,

$$U = 2.5 \sqrt{(\tau/\rho)} \log_e y + \text{constant}$$

$$\text{or } U = 5.75 \sqrt{(\tau/\rho)} \log_{10} y + \text{constant} \quad (10)$$

where  $U$  is the local velocity,  $y$  is the distance from the wall, and  $\tau$  is the shearing stress. If the slope  $S$  of the straight portion of the velocity-distribution curve plotted on semilogarithmic paper (fig. 10) is assumed to be equal to  $5.75 \sqrt{(\tau/\rho)}$ ,

$$\tau/\rho = S^2/33 \quad (11)$$

It is interesting to compare the shearing stress thus obtained with the values obtained by G. I. Taylor by means of torque measurement. (See reference 2.) Taylor plotted

$\log_{10}(\tau/\rho U^2)$  against  $\log_{10}(Ut/v)$  for various values of  $t/R_1$ , where  $\tau$  is the shearing stress on the outer cylinder,  $U = 2\pi NR_1$ ,  $N$  is the speed of rotation of the cylinder,  $R_1$  is the radius of the outer cylinder, and  $t$  is the gap distance between the two cylinders. It is correct to use the B-type velocity distribution for the comparison with Taylor's results because, in this case, the velocity profile is logarithmic near the outer cylinder wall. It is found that the difference of the shearing stress calculated from both walls is small, the shearing stress at the inner cylinder being a little larger than that at the outer cylinder. This result is to be expected. Figure 15 shows the comparison of the results. The full-line curve is an average curve obtained from Taylor's curves for  $t/R_1 = 0.0555$  and  $0.0776$ . Hence, it may be stated that this curve corresponds approximately to  $t/R_1 = 0.0666$ . This value compares with the curve obtained in the present investigation for  $t/R_1 = 0.0635$ . In addition, Taylor's curve for  $t/R_1 = 0.1146$  is compared with the present result for  $t/R_1 = 0.1190$ . It is seen that, for the large gap, the result of the present measurements checks Taylor's curve very well; whereas, for the small gap, the present results are higher than those obtained by Taylor. The general tendency that the coefficient of friction decreases with increasing value of  $t/R_1$  is found to be true.

#### CONCLUDING REMARKS

The turbulent flow between two coaxial cylinders is accompanied by a peculiar type of secondary motion that affects the transfer of momentum. The secondary flow can be described by assuming pairs of ring-shape vortices between the cylinders. The size and the number of the vortices depend on the speed of the inner rotating cylinder, the number tending to decrease with increasing speed. At certain critical speeds the flow pattern may suddenly change owing to the loss or the gain of a pair of vortices. There exist in the gap certain regions where the velocity distribution is governed mainly by this secondary flow and other regions where the turbulent fluctuations are predeterminant. In the regions in which the fluctuations are predeterminant, the velocity distribution is of the logarithmic type in agreement with the theory of homologous turbulence.

## REFERENCES

1. Taylor, G. I.: Stability of Viscous Liquid Contained between Two Rotating Cylinders. Phil. Trans. Roy. Soc. (London), vol. 223, Feb. 8, 1923, pp. 289-343.
2. Taylor, G. I.: Distribution of Velocity and Temperature between Concentric Rotating Cylinders. Proc. Roy. Soc. (London), ser. A, vol. 151, no. 874, Oct. 1, 1935, pp. 494-512.
3. Taylor, G. I.: Fluid Friction between Rotating Cylinders. Proc. Roy. Soc. (London), ser. A, vol. 157, no. 892, Dec. 2, 1936, pp. 546-578.
4. Wendt, F.: Turbulente Strömungen zwischen zwei rotierenden koaxialen Cylindern. Ing.-Archiv., Bd. IV, Heft 6, Sept. 1933, pp. 577-595.
5. von Kármán, Th.: Aspects of the Turbulence Problem. Proc. Fourth Int. Cong. Appl. Mech. (Cambridge, Eng., 1934) Cambridge Univ. Press, 1935, pp. 54-91.
6. von Kármán, Th.: The Fundamentals of the Statistical Theory of Turbulence. Jour. Aero. Sci., vol. 4, no. 4, Feb. 1937, pp. 131-138.



15

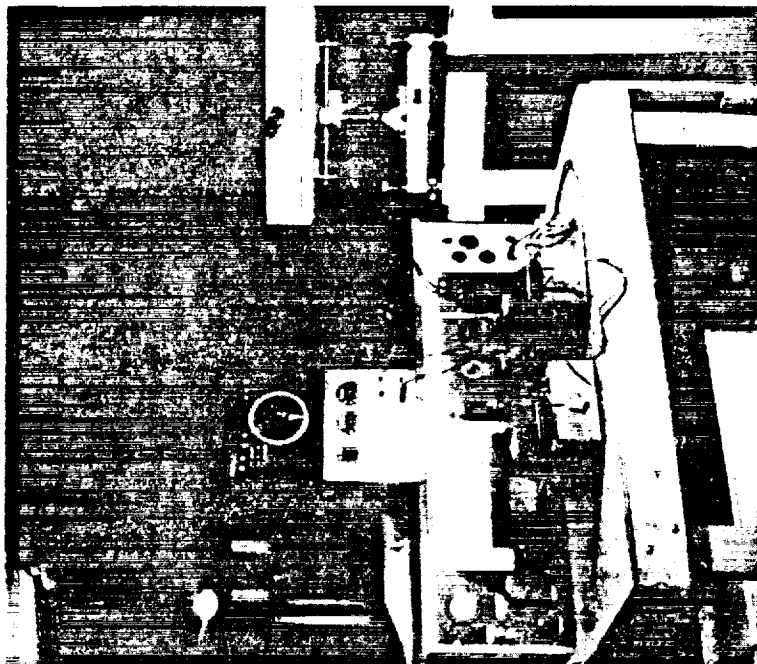


Figure 2.- The test setup for determining velocity distribution.

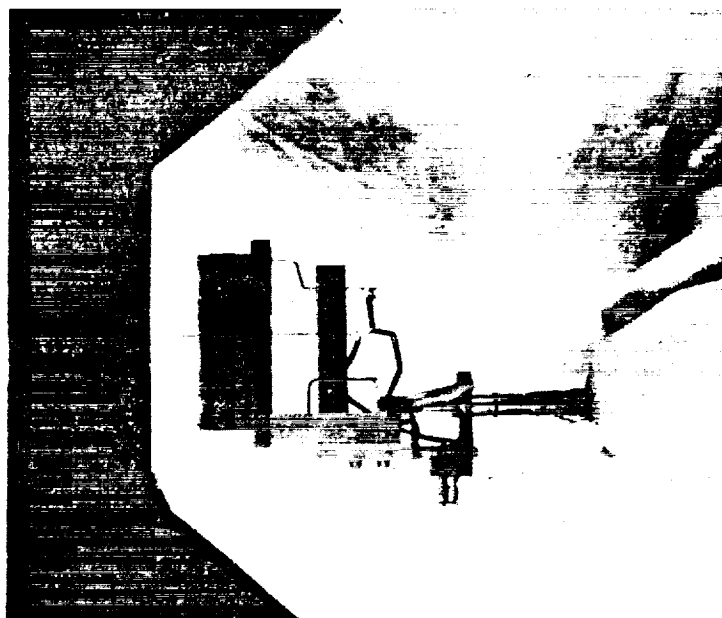


Figure 1.- Hot-wire holder, showing two hot wires used to measure simultaneously two axial stations.



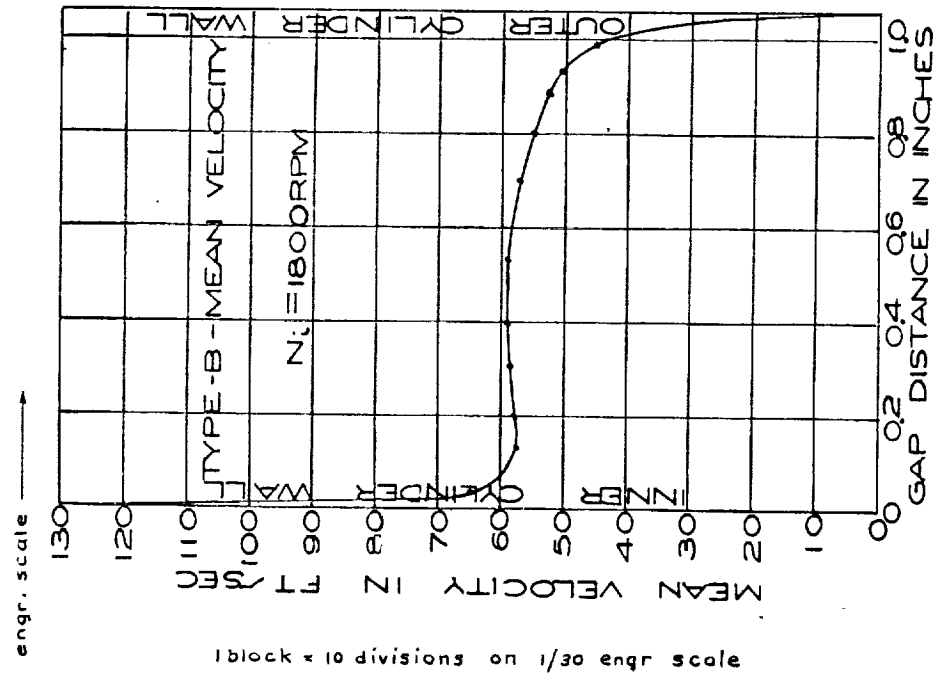


Figure 4.- Mean velocity distribution for type B flow.  $N_1$ , 1800 rpm.

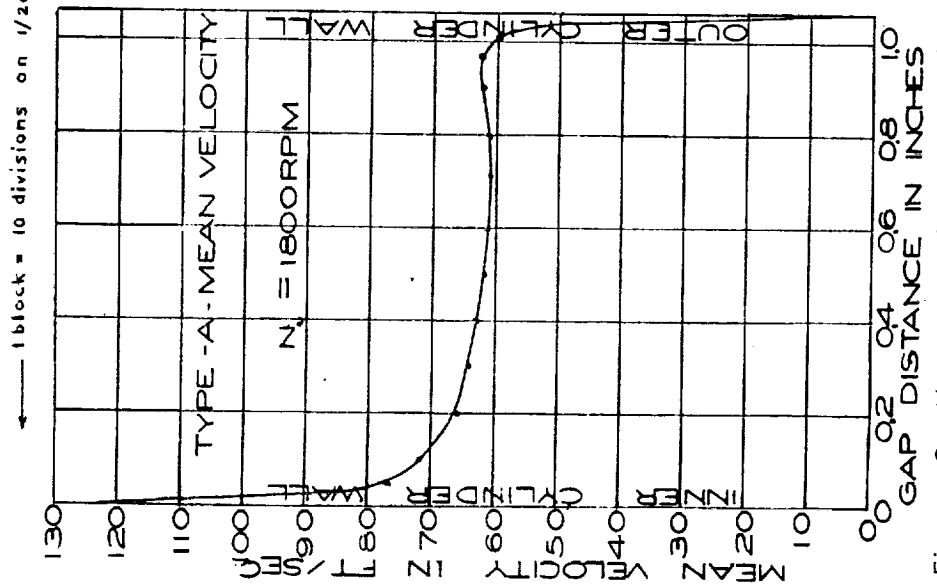


Figure 3.- Mean velocity distribution for type A flow.  $N_1$ , 1800 rpm.



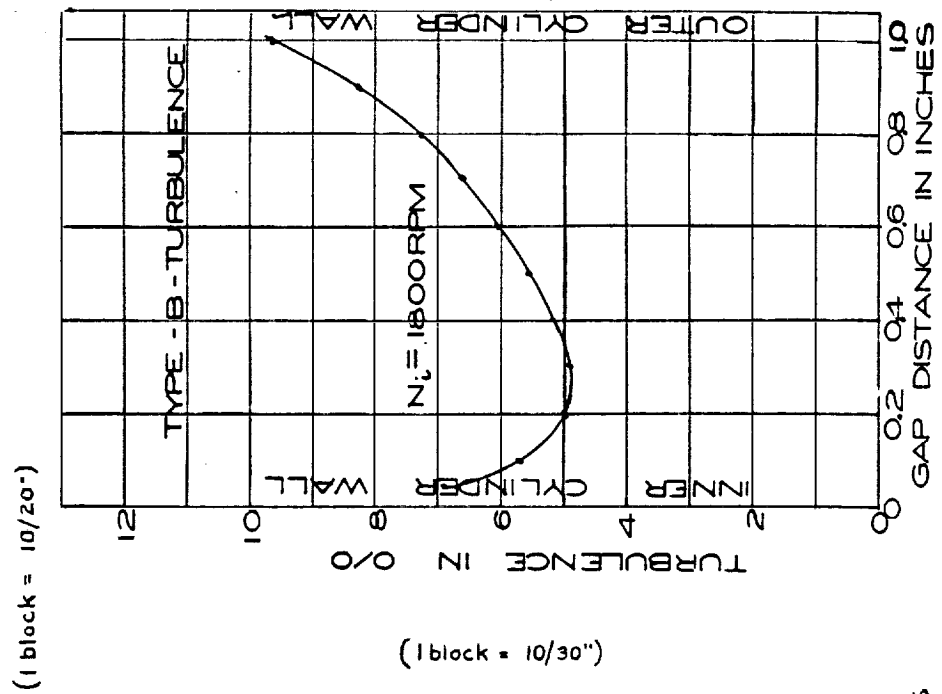


Figure 6.- Turbulence distribution for type B flow.  $N_i$ , 1800 rpm.

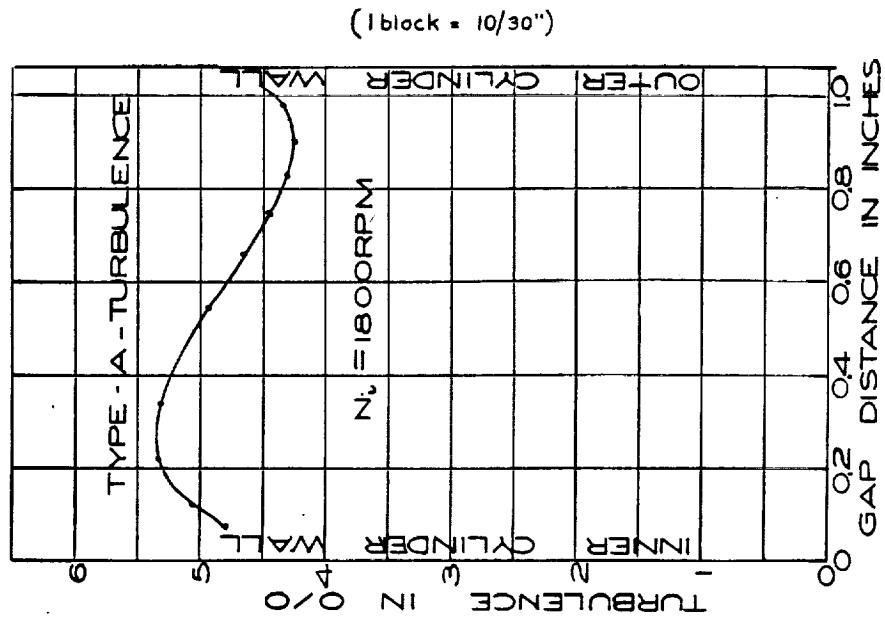


Figure 5.- Turbulence distribution for type A flow.  $N_i$ , 1800 rpm.



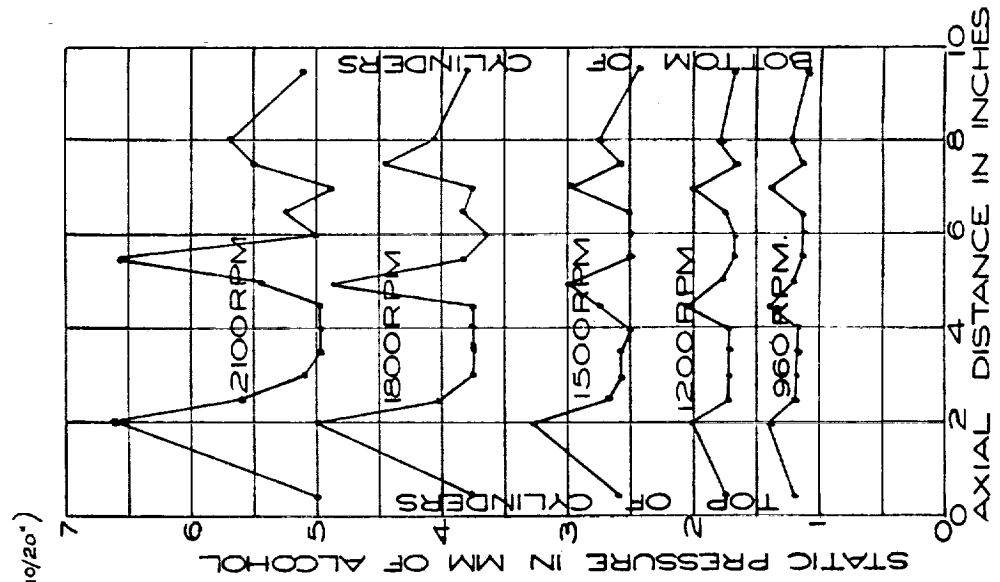


Figure 8.- Static-pressure measure along the outer cylinder.

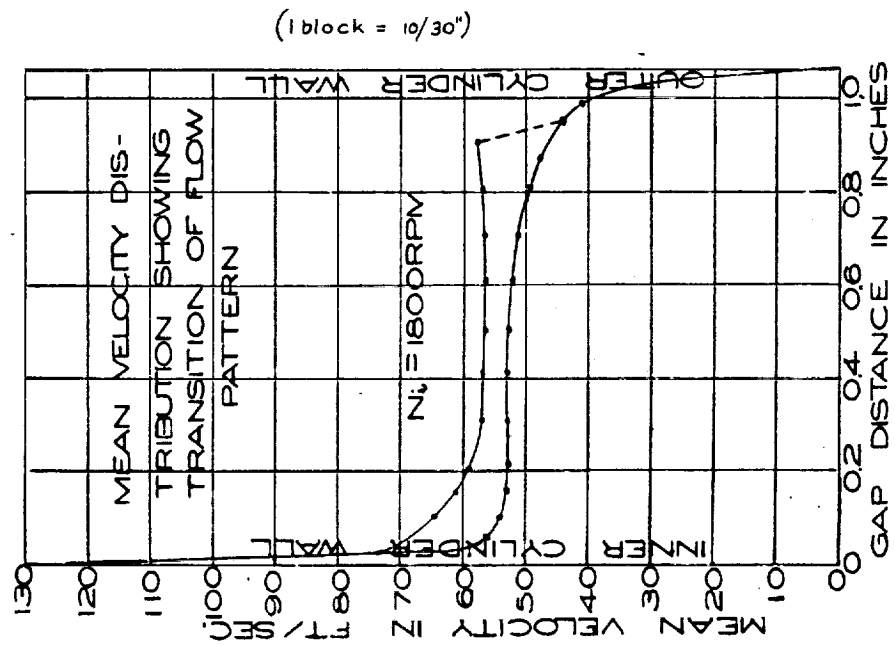
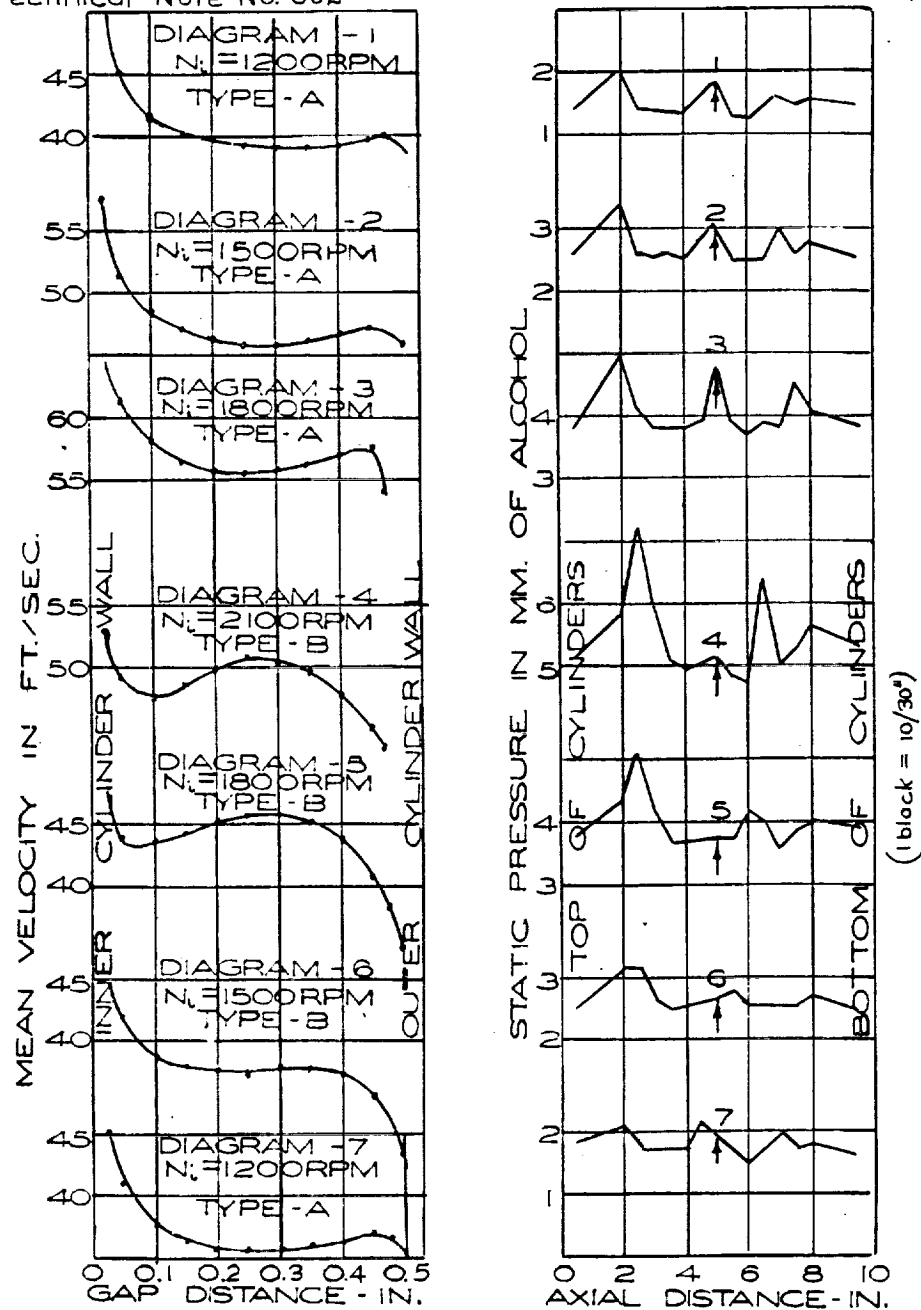


Figure 7.- Mean velocity distribution showing transition of flow pattern  $N_1$ , 1800 rpm.





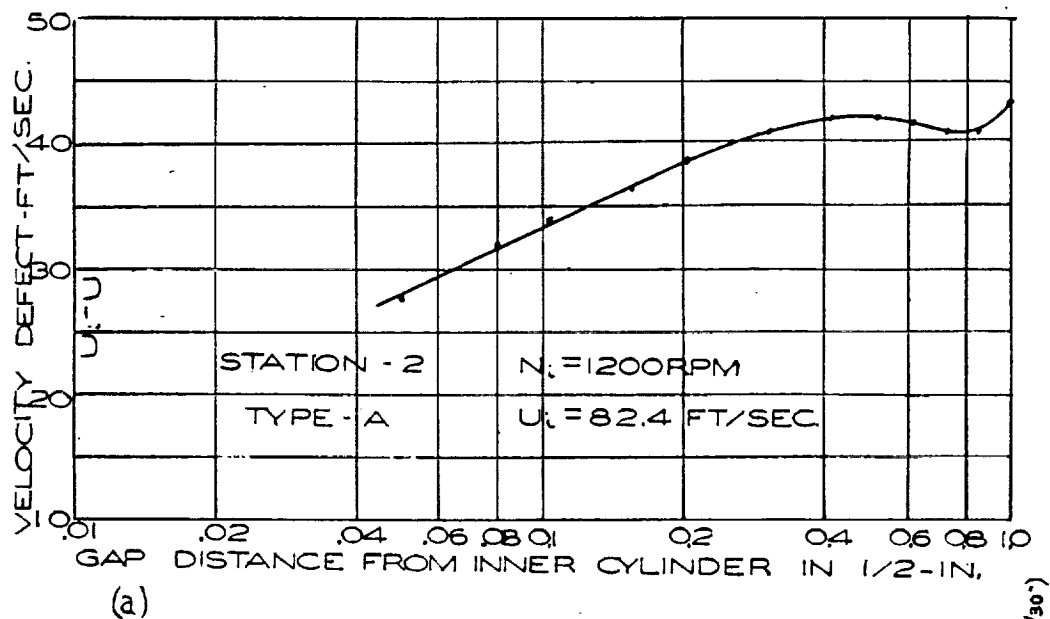


(a) Type A flow at station 2. (b) Type B flow at station 6.

Figure 9.- Mean velocity distribution and static pressure.

$N_i$ , 1200 rpm;  $U_i$ , 82.4 fps.





(1 block = 10/30°)

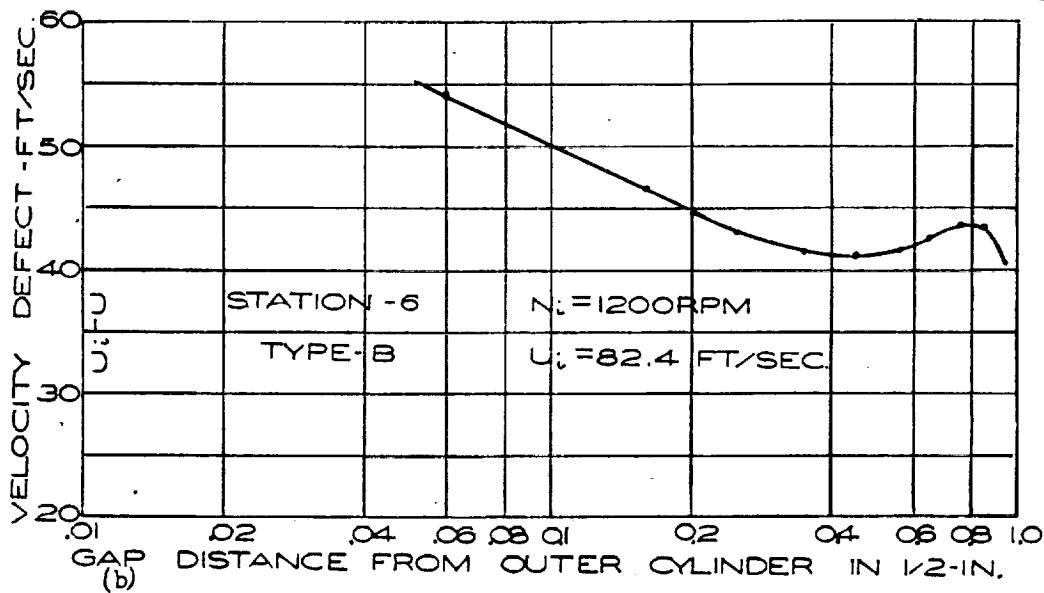


Figure 10.- Velocity defect between cylinders.  $N_i$ , 1200 rpm;  $U_i$ , 82.4 fps.



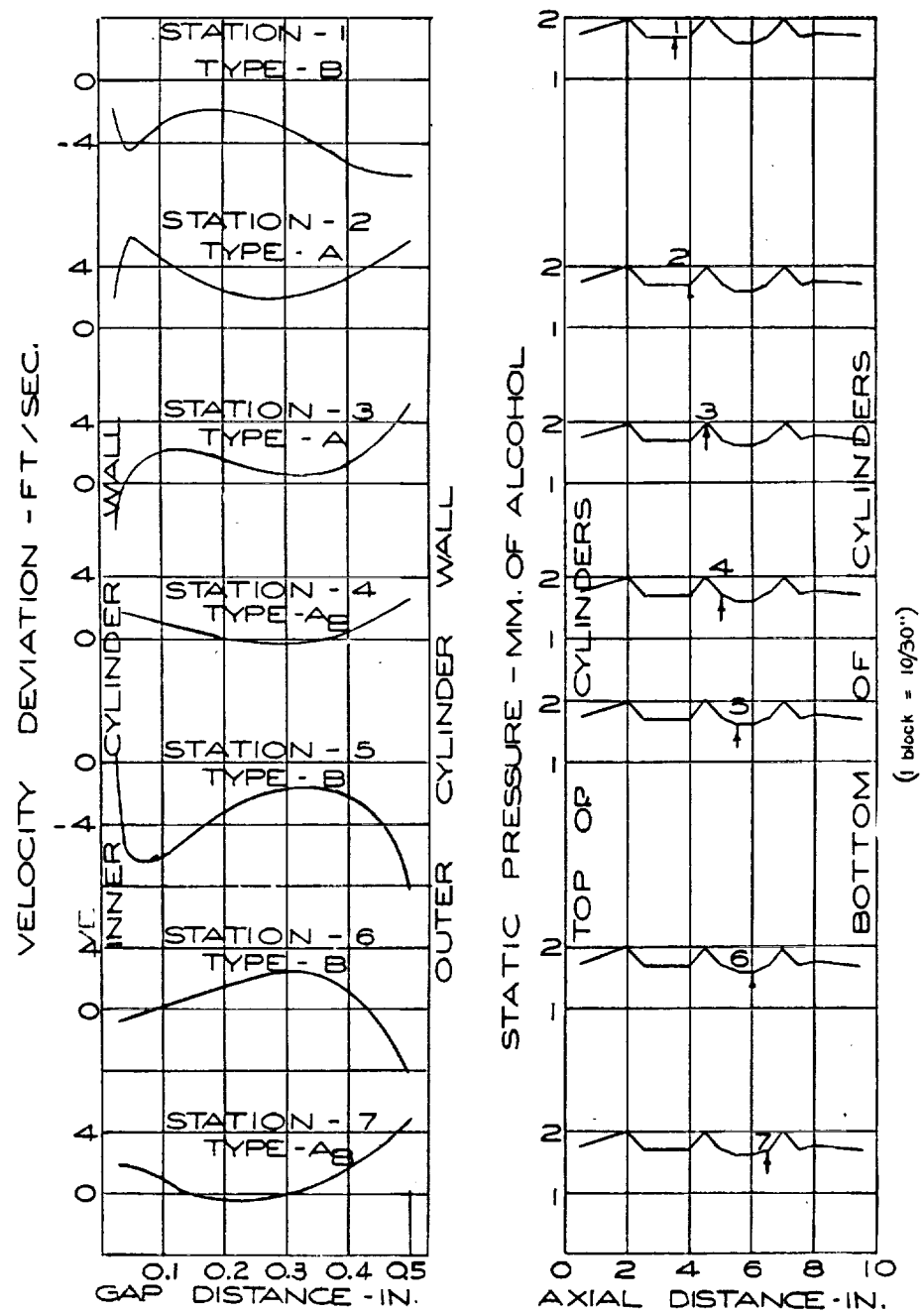


Figure 11.- Deviation from average velocity and static pressure for seven axial positions.



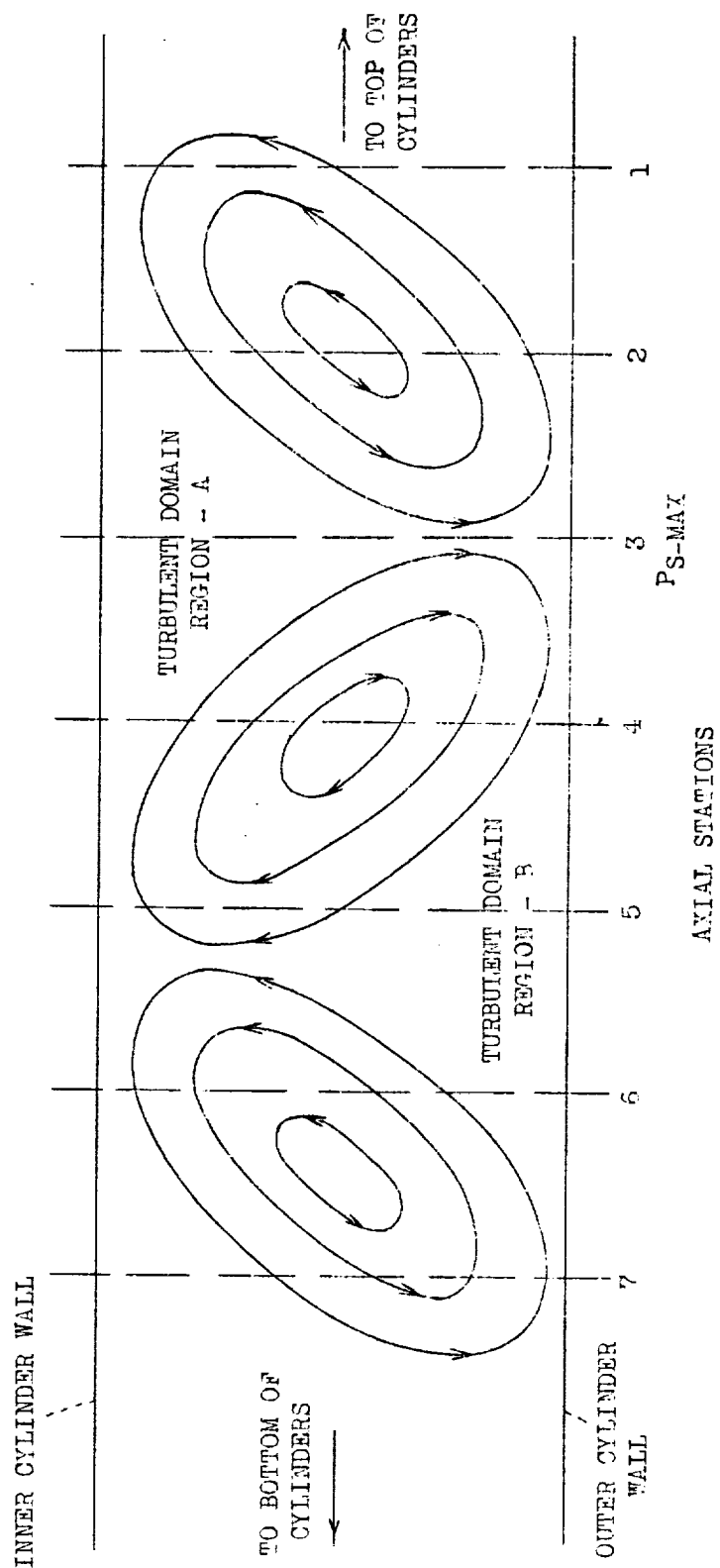


Figure 12.- Vortices between rotating cylinders.

221





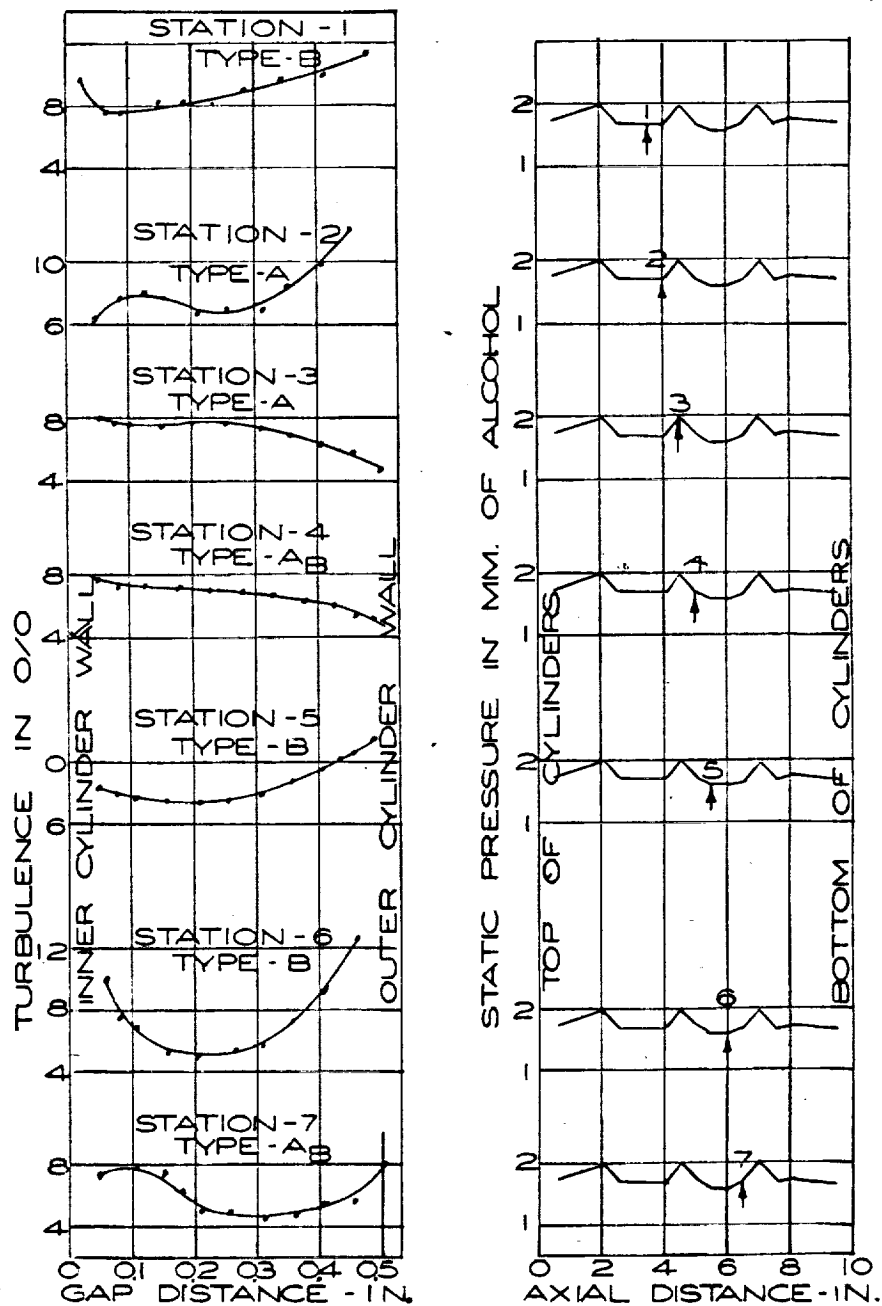


Figure 13.- Distributions of  $u'$ , the circumferential turbulent fluctuations, and static pressure for seven axial positions.



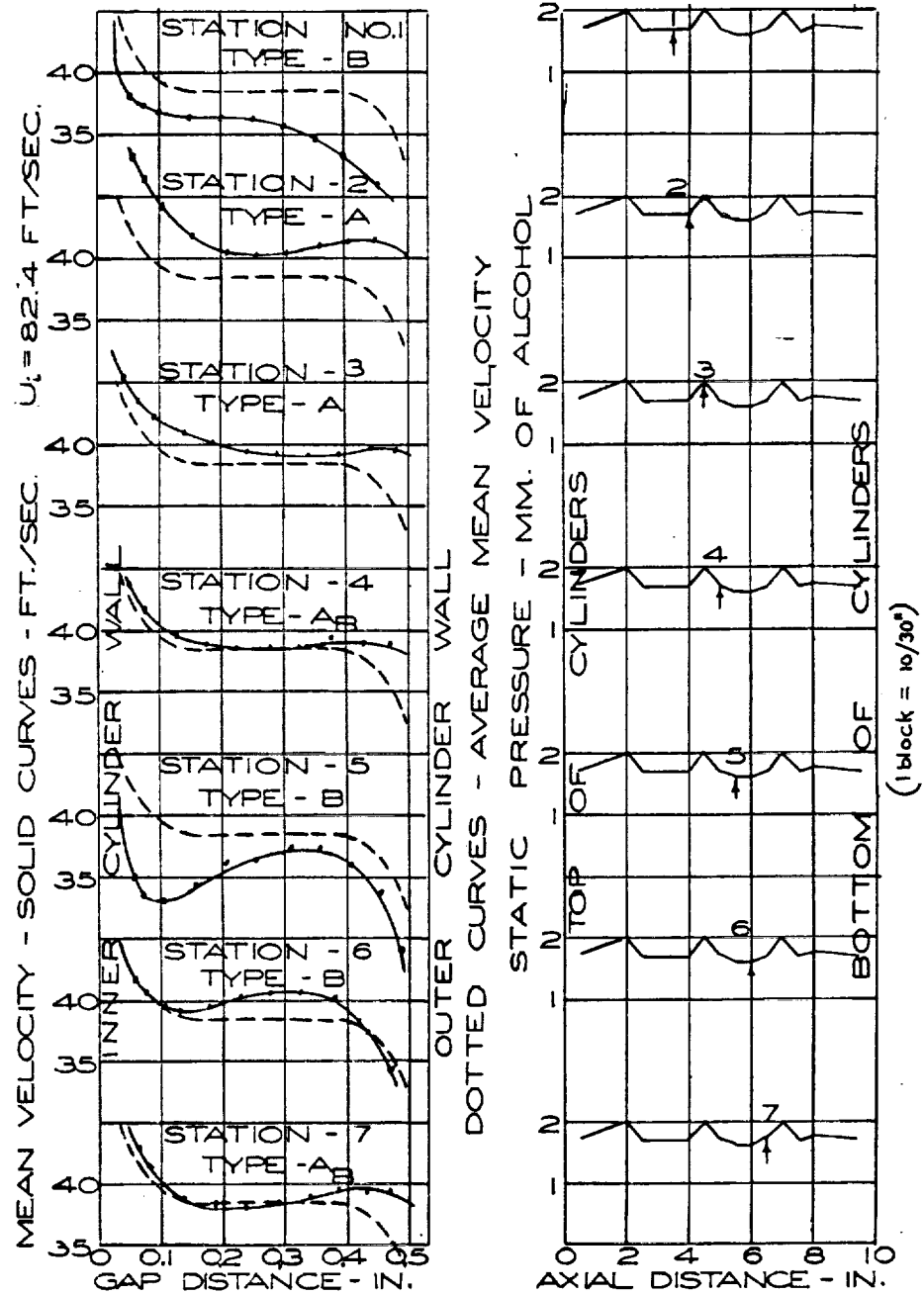


Figure 14.- Mean velocity distributions and static pressure at different rotating speeds for seven axial positions.



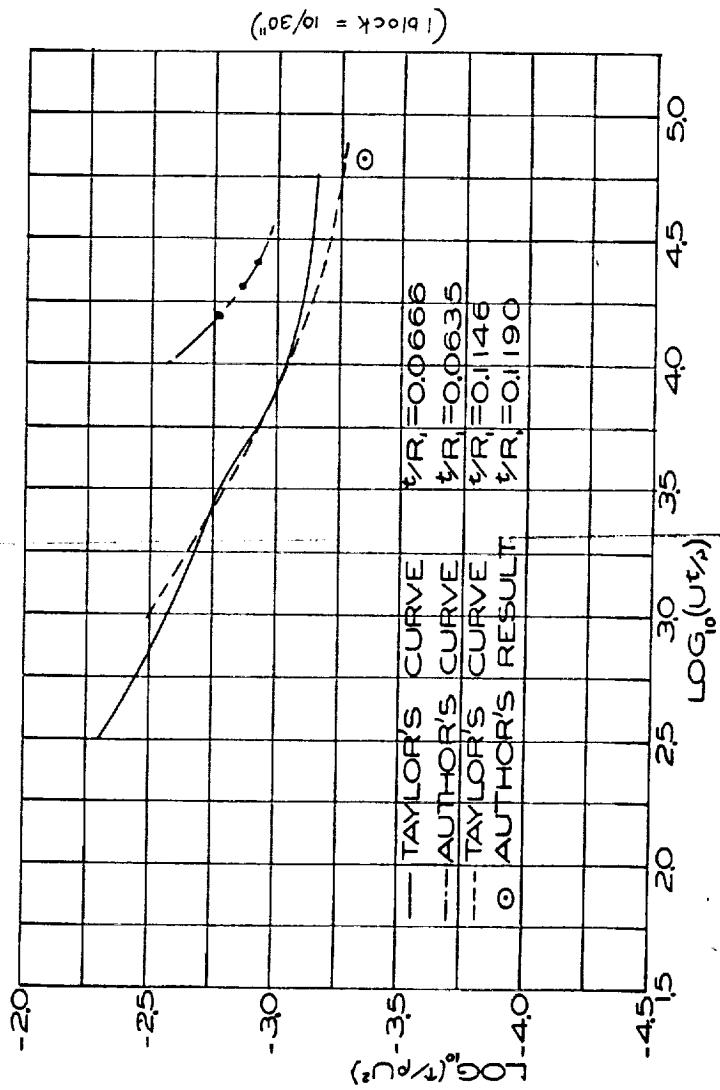


Figure 15.- Shearing stress diagram. Taylor's curves from reference 2.

